



A high-resolution regional emission inventory of atmospheric mercury and its comparison with multi-scale inventories: a case study of Jiangsu, China

Hui Zhong¹, Yu Zhao^{1,2*}, Marilena Muntean³, Lei Zhang⁴, Jie Zhang^{2,5}

1. State Key Laboratory of Pollution Control & Resource Reuse and School of the Environment, Nanjing University, 163 Xianlin Ave., Nanjing, Jiangsu 210023, China
2. Jiangsu Collaborative Innovation Center of Atmospheric Environment and Equipment Technology (CICAEET), Nanjing University of Information Science & Technology, Jiangsu 210044, China
3. European Commission, Joint Research Centre, Institute for Environment and Sustainability, Air and Climate Unit, Via E. Fermi, Ispra, Italy
4. University of Washington-Bothell, 18115 Campus Way NE, Bothell, WA 98011, U.S.A.
5. Jiangsu Provincial Academy of Environmental Science, 176 North Jiangdong Rd., Nanjing, Jiangsu 210036, China

* Corresponding author: Phone: 86-25-89680650; email: yuzhao@nju.edu.cn



1

ABSTRACT

2 A better understanding of the discrepancies in multi-scale inventories could give
3 an insight on their approaches and limitations, and provide indications for further
4 improvements; international, national and plant-by-plant data sources are primarily
5 obtained to compile those inventories. In this study we develop a high-resolution
6 inventory of Hg emissions at $0.05^\circ \times 0.05^\circ$ for Jiangsu China using a bottom-up
7 approach and then compare the results with available global/national inventories. With
8 detailed information on individual sources and the updated emission factors from field
9 measurements incorporated, the annual Hg emissions of anthropogenic origin in
10 Jiangsu 2010 are estimated at 39 105 kg, of which 51%, 47% and 2% were released as
11 Hg^0 , Hg^{2+} , and Hg^{P} , respectively. This provincial inventory is thoroughly compared to
12 the downscaled results from three national inventories (NJU, THU and BNU) and two
13 global inventories (AMAP/UNEP and EDGARv4.tox2). Attributed to varied methods
14 and data sources, clear information gaps exist in multi-scale inventories, leading to
15 differences in the emission levels, speciation and spatial distributions of atmospheric
16 Hg. The total emissions in the provincial inventory are the largest, i.e., 28%, 7%, 19%,
17 22%, and 70% higher than NJU, THU, BNU, AMAP/UNEP, and EDGARv4.tox2,
18 respectively. For major sectors including power generation, cement, iron & steel and
19 other coal combustion, the Hg contents (HgC) in coals/raw materials, abatement rates
20 of air pollution control devices (APCD) and activity levels are identified as the crucial
21 parameters responsible for the differences in estimated emissions between inventories.
22 Regarding speciated emissions, larger fraction of Hg^{2+} is found in the provincial
23 inventory than national and global inventories, resulting mainly from the results by
24 the most recent domestic studies in which enhanced Hg^{2+} were measured for cement
25 and iron & steel plants. Inconsistent information of big power and industrial plants is
26 the main source of differences in spatial distribution of emissions between the
27 provincial and other inventories, particularly in southern and northwestern Jiangsu
28 where intensive coal combustion and industry are located. Quantified with
29 Monte-Carlo simulation, uncertainties of provincial Hg emissions are smaller than
30 those of NJU national inventory, resulting mainly from the more accurate activity data
31 of individual plants and the reduced uncertainties of HgC in coals/raw materials.



32

1 INTRODUCTION

33 Mercury (Hg), known as a global pollutant, has received increasing attention for
34 its toxicity and long-range transport. Identified as the most significant release into the
35 environment (Pirrone and Mason, 2009; AMAP and UNEP, 2013), atmospheric Hg is
36 analytically defined as: gaseous elemental Hg (GEM, Hg^0) that has longest lifetime
37 and transport distance, and reactive gaseous mercury (RGM, Hg^{2+}) and particle-bound
38 mercury (PBM, Hg^p) that are more affected by local sources. Improved estimates in
39 emissions of speciated atmospheric Hg are believed to be essential for better
40 understanding the global transport, chemical behaviors and mass balance of Hg.

41 Due mainly to the fast growth in economy and intensive use of fossil fuels, China
42 has been indicated as the highest ranking nation in anthropogenic Hg emissions (Fu et
43 al., 2012; Pacyna et al., 2010; Pirrone et al., 2010). Emissions of speciated
44 atmospheric Hg of anthropogenic origin in China have been estimated at both global
45 and national scales. For example, AMAP/UNEP (2013) and Muntean et al. (2014)
46 developed global Hg inventories, with national-specific emissions reported for China
47 for 2010 and from 1970 to 2008, respectively. At national scale, Hg emissions have
48 been estimated based on more detailed provincial information on energy consumption
49 and industrial production. Zhang et al. (2015), Zhao et al. (2015a) and Tian et al.
50 (2015) evaluated the inter-annual trends in emissions for 2000-2010, 2005-2012, and
51 1949-2012, respectively, to explore the benefits of air pollution control polices,
52 particularly for recent years.

53 There are considerable information gaps between multi-scale inventories,
54 attributed mainly to the data of different sources and levels of details. For coal-fired
55 power plants (CPP), as an example, the global inventories by AMAP/UNEP (2013)
56 and Muntean et al. (2014) obtained the national coal consumption from the
57 International Energy Agency (IEA), and they acquired the information of control
58 technologies from the “national comments” by selected experts and World Electric
59 Power Plants database (WEPP), respectively. In the national inventory by Zhang et al.
60 (2015) and Tian et al. (2015), coal consumption of CPP by province was derived from
61 official energy statistics, and the penetrations of flue gas desulfurization (FGD)
62 systems were assumed at provincial level. Zhao et al. (2015a) further analyzed the
63 activity data and emission control levels plant by plant using a “unit-based” database
64 of power sector. Although data of varied sources and levels of details result in



65 discrepancies between inventories, those discrepancies and the underlying reasons
66 have not been thoroughly analyzed in previous studies, leading to big uncertainty in
67 Hg emission estimation.

68 Existing global and national inventories could hardly provide satisfying estimates
69 in speciated Hg emissions or well capture the spatial distribution of emissions at
70 regional/local scales, attributed mainly to relatively weak investigation on individual
71 sources. When they are used in chemistry transport model (CTM), downscaled
72 inventories at global/national scales would possibly bias the simulation at smaller
73 scales. Improvement in emission estimation at local scale, particularly for the large
74 point sources is thus crucial for better understanding the atmospheric processes of Hg
75 (Lin et al., 2010; Wang et al., 2014; Zhu et al., 2015). While local information based
76 on sufficient surveys is proven to have advantages in improving the emission
77 estimates for given pollutants like NO_x and PM₁₀ (Zhao et al., 2015b; Timmermans et
78 al., 2013), there are currently very few studies focusing on Hg at regional/local scales,
79 and the differences of multi-scale inventories remain unclear.

80 In this work, therefore, we select Jiangsu, one of the most developed provinces
81 with serious air pollution in China, as study area. Firstly, we develop a high-resolution
82 Hg emission inventory of anthropogenic origin for 2010, based on comprehensive
83 review of field measurements and detailed information on emission sources. That
84 provincial inventory is then compared to selected global and national inventories with
85 a thorough analysis on data and methods of multi-scale inventories. Discrepancies in
86 emission levels, speciation, and spatial distributions are evaluated and the underlying
87 sources of the discrepancies are figured out. Finally, the uncertainty of the provincial
88 emission inventory is quantified and the key parameters contributing to the
89 uncertainty are identified. The results provide an insight on the effects of varied
90 approaches and data on development of Hg emission inventory, and indicate the
91 limitations of current studies and the orientations for further improvement on emission
92 estimation at regional/local scales.

93

94

2 DATA AND METHODS

2.1 Data sources of multi-scale inventories

95 As shown in Figure S1 in the supplement, Jiangsu province (30°45' N-35°20' N,
96 116°18' E-121°57' E) is located in Yangtze River Delta in eastern China and covers 13
97



98 cities. The Hg emissions of Jiangsu are obtained from two approaches: downscaled
99 from global/national inventories, and estimated using a bottom-up method with
100 information of local sources incorporated.

101 In global/national inventories, Hg emissions were first calculated by sector based
102 on activity data and emission factors that were obtained or assumed at global, national
103 or provincial level, and were then downscaled to regional domain with finer spatial
104 resolution. Various methods and data were adopted in multi-scale inventories to
105 estimate Hg emissions for different sectors, as summarized briefly in Table S1 in the
106 supplement. Three national inventories were developed by Nanjing University (NJU,
107 Zhao et al., 2015a), Beijing Normal University (BNU, Tian et al., 2015), and Tsinghua
108 University (THU, Zhang et al., 2015), with major activity data at provincial level
109 obtained from Chinese national official statistics. Compared to NJU and BNU
110 inventories that applied deterministic parameters relevant to emission factors, THU
111 developed a model with probabilistic technology-based emission factors to calculate
112 the emissions. Based on international activity statistics at national level, two global
113 inventories for 2010 were developed by the joint expert group of Arctic Monitoring
114 and Assessment Programme and United Nations Environment Programme
115 (AMAP/UNEP, 2013), and Emission Database for Global Atmospheric Research
116 (EDGARv4.tox2, unpublished). AMAP/UNEP inventory developed a new system for
117 estimating emissions from main sectors based on a mass-balance approach with data
118 on unabated emission factors and emission reduction technology employed in
119 different countries. EDGARv4.tox2 inventory calculated the emissions for all the
120 countries by primarily applying emission factors from EEA (2009) and USEPA (2012),
121 combined with regional technology-specific information of emission abatement
122 measures.

123

124 **2.2 Development of the provincial inventory**

125 In contrast to the downscaling approach, a bottom-up method is further applied,
126 in which the emissions are first calculated plant by plant based on information of
127 individual sources and then aggregated at provincial level. We mention the inventory
128 as bottom-up or provincial inventory hereinafter. Information for individual sources
129 are thoroughly collected from Pollution Source Census (PSC, internal data from
130 Environmental Protection Agency of Jiangsu Province), including combustion
131 technology, fuel quality and air pollutant control devices. According to the availability



132 of data, anthropogenic sources are classified into three main categories. Category 1
 133 includes coal-fired power plants (CPP), iron & steel plants (ISP), cement production
 134 (CEM) and other industrial coal combustion (OIB). Note that the emissions from coal
 135 combustion in cement production are not included in CEM but in OIB, following
 136 most other inventories involved in this work for easier comparison. The information
 137 on geographic location, activity levels (consumption of energy or raw materials) and
 138 penetration of air pollution control devices (APCDs) is compiled plant by plant from
 139 Pollution Source Census, with an exception that the technology employed in CEM are
 140 obtained from CCA (2011). Category 2 includes nonferrous metal smelting (NMS),
 141 aluminum production (AP), municipal solid waste incineration (MSWI) and
 142 intentional use sector (IUS: thermometer, fluorescent lamp, battery and polyvinyl
 143 chloride polymer production). Geographic location information for those sources is
 144 obtained from Pollution Source Census, while other activity data come from official
 145 statistics at provincial level. Category 3 includes emission sources that are not
 146 contained in Pollution Source Census: residential & commercial coal combustion
 147 (RCC), oil & gas combustion (O&G), biofuel use/biomass open burning (BIO), rural
 148 solid waste incineration (RSWI) and human cremation (HC). They are defined as area
 149 sources, and the data sources for them are discussed later in this section.

150 In general, annual emissions of total and speciated Hg are calculated using Eq. (1)
 151 and (2), respectively:

$$E = \sum_n AL_n \times EF_n \quad (1)$$

$$E_s = \sum_n AL_n \times EF_n \times F_{n,s} \quad (2)$$

152 where E is the Hg emission; AL is the activity levels (fuel consumption or industrial
 153 production); EF is the combined emission factor (emissions per unit of activity level);
 154 F is the mass fraction of given Hg speciation; n and s represent emission source type
 155 and Hg speciation (Hg^0 , Hg^{2+} or Hg^p).

156 For CPP/OIB and CEM, Eq. (1) can be revised to Eq. (3) and (4) respectively,
 157 with detailed fuel and technology information of individual sources incorporated:

$$E_{CPP/OIB} = \sum_t \sum_i \sum_k AL_{t,i,k} \times HgC_k \times RR_{t,i} \times (1 - RE_t) \quad (3)$$

$$E_{CEM} = \sum_t \sum_i (AL_{Limstone} \times HgC_{Limstone} + AL_{Other,i} \times HgC_{Other}) \times (1 - RE_t) \quad (4)$$

158 where HgC is the Hg content of coal consumed in Jiangsu, calculated based on



159 measured Hg contents of coal mines across the country and an inter-provincial flow
160 model of coal transport (Zhang et al., 2015); $HgC_{Limestone}$ and HgC_{Other} represent Hg
161 contents of limestone and other raw materials (e.g. malmstone and iron powder) in
162 cement production, respectively; RR is the Hg release ratios from combustors; RE is
163 Hg removal efficiency of APCDs; $AL_{Limestone}$ and AL_{Other} represent the consumption of
164 limestone and other raw materials in CEM, respectively; i and k represent individual
165 point source and coal type, respectively; t represent APCD type including wet
166 scrubber (WET), cyclone (CYC), fabric filter (FF), electrostatic precipitator (ESP),
167 FGD and selective catalyst reduction (SCR) systems for CPP, and dry-process
168 precalciner technology with dust recycling (DPT+DR), shaft kiln technology (SKT)
169 and rotary kiln technology (RKT) with ESP or FF for CEM. Note the AL for
170 individual CEM plant is calculated based on the clinker and cement production when
171 the information on limestone or other raw materials is missing in PSC.

172 For ISP, Eq. (1) could be revised to Eq. (5):

$$E_{ISP} = \sum_i (AL_{steel,i} + AL_{iron,i} \times R) \times EF_{steel} \quad (5)$$

173 where AL_{steel} and AL_{iron} represent crude steel and pig iron production in ISP,
174 respectively; R is the liquid steel to hot metal ratio provided by BREF (2012),
175 converting the production of pig iron to crude steel equivalent; EF_{steel} is the Hg
176 emission factor applied to steel making, obtained from recent domestic tests by Wang
177 et al. (2016).

178 Activity data for NMS, AP, MSWI, RCC and O&G are derived from national
179 statistics (NMIA, 2011; NSB, 2011a; 2011b), while Hg consumption in IUS are
180 estimated based on the internal industry reports. The biofuel use is obtained from the
181 investigation by Ministry of Agriculture (C. Chen et al., 2013). The biomass
182 combusted in open fields is originally calculated as a product of grain production,
183 waste-to-grain ratio, and the percentage of residual material burned in the field, as
184 described in Zhao et al. (2011, 2012). The rural municipal waste burned are calculated
185 as a product of rural population, the average waste per capita, and the ratios of waste
186 that is burned (Yao et al., 2009). Other information including control efficiencies of
187 APCDs, speciation profiles and emission factors inherited from previous studies is
188 summarized in Table S2-S4 in the supplement.

189 Regarding the spatial pattern of emissions, the study domain is divided into 4212
190 grid cells with a resolution at $0.05^\circ \times 0.05^\circ$. For Categories 1 and 2, emissions are



191 directly allocated into corresponding grid cells according to the locations of individual
192 sources. As considerable errors of plant locations were unexpectedly found in PSC,
193 the geographic location for point sources with emissions more than 15 kg have been
194 corrected by Google Map. As a result, totally 900 plants are relocated, accounting for
195 14% of all the point sources. For Category 3, emissions are allocated according to the
196 population density in urban areas (RCC) and that in rural areas (BIO and RSWI).

197

198 **2.3 Sensitivity and uncertainty analysis**

199 For better understanding the sources of discrepancies between inventories, a
200 comprehensive sensitivity analysis is conducted to quantify the differences between
201 selected parameters used in multi-scale inventories and the subsequent changes in
202 emission estimation for Category 1 sources. The relatively change (RC) of given
203 parameter (j) in global/national inventories compared to those in the provincial
204 bottom-up inventory, and the changes in Hg emissions for selected source (n) when
205 the value of given parameter in the bottom-up inventory is replaced by that in
206 global/national inventories ($E_{diff,n}$), can be calculated using Eqs. (6) and (7),
207 respectively:

$$RC_j = (VO_j - VB_j) / VB_j \quad (6)$$

$$E_{diff,n} = EO_n - EB_n \quad (7)$$

208 where VB is the value of parameters in bottom-up inventory; VO is the value of
209 parameters in other national/global inventories; EB is Hg emissions for given sector in
210 bottom-up inventory; EO is Hg emissions for given sector when the values of
211 parameters in bottom-up inventory are replaced by those in other global/national
212 inventories; j and n represent given parameter and source type, respectively.

213 In particular, a new parameter, total abatement rate (TA), is defined for the
214 sensitivity analysis, combining the effect of the penetrations of APCDs and their
215 removal efficiencies on emission abatement:

$$TA = \sum_t AR_t \times RE_t \quad (8)$$

216 where t represents APCD type; AR and RE are the application rate and Hg removal
217 efficiency, with detailed information provided in Table S5 in the supplement.

218 The uncertainties of speciated Hg emissions at provincial level are quantified
219 using a Monte-Carlo framework (Zhao et al., 2011). Given the relatively accurate data



220 reported in PSC, the probability distributions of activity levels for individual plants of
221 CPP, OIB, ISP and CEM are defined as normal distributions with the relative standard
222 deviations (RSD) set at 10%, 20%, 20% and 20% respectively. As summarized in
223 Table S6 and Table S7 in the supplement, a database for Hg emission factors/related
224 parameters by sector and speciation for main sources are established for China, with
225 the uncertainty analyzed and presented by probability distribution function (PDF).
226 The PDFs of Hg contents in coal mines by province are obtained from Zhang et al.
227 (2015). For Hg content in limestone ($HgC_{Limestone}$), a lognormal distribution is
228 generated with bootstrap simulation based on 17 field tests by Yang (2014), as shown
229 in Figure S2 in the supplement. For the rest parameters, a comprehensive analysis of
230 uncertainties were conducted with the results of field measurements available fully
231 incorporated as described in Zhao et al. (2015a). Ten thousand simulations are
232 performed to estimate the uncertainties of emissions, and the parameters that are most
233 significant in determination of the uncertainties are identified by source type
234 according to the rank of their contributions to variance.

235

236

3 RESULTS AND DISCUSSIONS

237 3.1 Emission estimation and comparison by sector

238 3.1.1 The total Hg emissions from multi-scale inventories

239 Table 1 provides the Hg emissions by sector and species for Jiangsu 2010
240 estimated from the bottom-up approach. The provincial total Hg emissions of
241 anthropogenic origin are calculated at 39 105 kg, of which 51% released as Hg^0 , 47%
242 as Hg^{2+} , and 2% as Hg^P . In general, Categories 1, 2 and 3 account for 90%, 4% and
243 6% of the total emissions, respectively. CPP and CEM are the biggest
244 contributors to the total Hg (Hg^T) emissions. For Hg^0 , Hg^{2+} , and Hg^P , the sectors with
245 the largest emissions are CPP, CEM, and OIB respectively.

246 To better understand the discrepancies and their sources between various studies,
247 the emissions from multi-scale inventories are also summarized in Table 1 for
248 comparison. Among all the inventories, the total emissions in the provincial inventory
249 are the largest, i.e., 28%, 7%, 19%, 22%, and 70% higher than NJU, THU, BNU,
250 AMAP/UNEP, and EDGARv4.tox2, respectively. The elevated Hg emissions
251 compared to previous studies could be supported by modeling and observation work



252 to some extent. Based on the chemistry transport modeling using GEOS-Chem (Wang
253 et al., 2014), or correlation slopes with certain tracers (CO, CO₂ and CH₄) from
254 ground observation (Fu et al., 2015), underestimation was suggested for the regional
255 Hg emissions of anthropogenic origin in China.

256 Direct comparison of emissions between inventories is unavailable for every
257 sector, as the definition of source categories is not fully consistent with each other.
258 Therefore, necessary assumption and modification are made on source classification
259 for global inventories. In Table 1, CPP, OIB and RCC for EDGARv4.tox2 actually
260 represent the emissions for all the fossil fuel types, and they are 1316, 5342 lower and
261 986 kg higher than our estimation from coal combustion, respectively. For
262 AMAP/UNEP, the emissions from regrouped stationary combustion (industrial
263 sources excluded), industry, and intentional use and product waste associated sources
264 (see Table 1 for the detailed definition) are respectively 3382, 2032 higher and 3118
265 kg lower than our estimation with bottom-up method. Figure 1 shows the ratios of the
266 estimated Hg emissions in national/global inventories to those in the provincial
267 inventory by source. The CPP emissions are relatively close to each other, but larger
268 differences exist in some other sources. The estimates for CEM and ISP in provincial
269 inventory are much higher than NJU, BNU and EDGARv4.tox2 inventories, while
270 those for NMS are extremely smaller. The reasons for those differences are discussed
271 and analyzed in details in Sections 3.1.2 and 3.1.3.

272 **3.1.2 Sensitivity analysis for Category 1 sources**

273 Figure 2 (a) and (b) represents the relative changes in given parameters between
274 the provincial and other inventories, and the subsequent differences in Hg emissions
275 for Category 1 sources, using Eqs. (6) and (7), respectively. For CPP, the differences
276 between provincial and national/global inventories are mainly determined by *AL*, *HgC*,
277 *TA*, and *IEF*, as indicated by the calculation methods summarized in Table S1.
278 (Instead of analyzing *HgC* and *RR* separately, integrated input emission factors (*IEF*)
279 were applied in AMAP/UNEP and EDGARv4.tox2.) For activity level (*AL*), the
280 coal consumption data are collected and compiled plant by plant in the provincial
281 inventory, while they were obtained from Chinese official statistics (NSB, 2011b) in
282 national inventories. As a result, the coal consumptions in NJU and THU inventories
283 are 17% and 6% smaller than our provincial inventory, resulting in 1968 and 760 kg
284 reduction in Hg emission estimate, respectively.



285 In national and provincial inventories, as mentioned in Section 2, the Hg contents
286 in the raw coal (HgC_{raw}) consumed by province are estimated using an
287 inter-provincial flow matrix for coal transport based on the results of field
288 measurements on Hg contents for given coal mines (Tian et al., 2010; Tian et al., 2014;
289 Zhang et al., 2012). The HgC_{raw} for Jiangsu in THU and our provincial inventory
290 come from Zhang et al. (2012), who merged the results of two comprehensive
291 measurement studies on HgC_{raw} for coal mines across China after 2000, by
292 themselves and USGS (2004), and the average value is calculated at 0.2 g/t-coal. NJU
293 inventory adopted the HgC_{raw} of 0.169 g/t-coal from Tian et al. (2010), while BNU
294 inventory determined HgC_{raw} at 0.25 g/t-coal with a bootstrap simulation based on a
295 thorough investigation on published data (Tian et al., 2014). HgC_{raw} in NJU and BNU
296 inventories are 15% smaller and 25% higher than that in provincial inventory, leading
297 to differences of 1746 and 2816 kg in Hg emissions, respectively. Given the large
298 differences in HgC_{raw} between countries, global inventories applied national specific
299 IEF based on the domestic tests (UNEP, 2011b; Wang et al., 2010). The IEFs for
300 China applied in AMAP/UNEP and EDGARv4.tox2, without considering the
301 regional differences in HgC_{raw} , are 26% and 28% lower than that in provincial
302 inventory (recalculated with HgC_{raw} and RR). As regional HgC_{raw} differs a lot from
303 the national average and could be largely influenced by the data selected, big
304 discrepancy might exist when national value is applied in regional inventory, and
305 more regional-specific measurements are suggested for constraining the uncertainty.

306 Total abatement rate (TA) of APCDs installed for CPP is calculated at 57% in the
307 provincial inventory, 6.7 % and 8.2% smaller than that in THU and AMAP/UNEP
308 inventories, respectively, and 12% larger than that in NJU inventory. The differences
309 result mainly from the varied removal efficiencies (RE) and application ratios (AR), as
310 shown in Table S5. For RE , local tests on FF, ESP+FGD and SCR+ESP+FGD were
311 conducted by JSEMC (2013) and Xie and Yi (2014), and the results (provided in
312 Table S2) are applied in the provincial inventory. From investigation on individual
313 plants, the AR of FGD systems with relatively large benefits on Hg removal was
314 underestimated in NJU and overestimated in THU inventory. In the AMAP/UNEP
315 inventory, relevant parameters were obtained from national comment, and elevated TA
316 was estimated due to the larger AR of FF and FGD and the higher RE of FGD+ESP
317 compared to those obtained from detailed source investigation in the provincial
318 inventory.



319 For OIB, the comparison of HgC is similar to that for CPP. AL from PSC in
320 provincial inventory is very close to that in THU inventory obtained from NSB
321 (2011b), while AL in NJU inventory was much lower as the coal consumption of
322 CEM and ISP were excluded. The RR from industrial boilers in this work is estimated
323 at 82% based on domestic measurements (Wang et al., 2000; Tang et al., 2004), much
324 lower than the result in THU inventory measured by Zhang et al. (2012), i.e., 95% for
325 stoker fired boiler. Given the limited samples in both inventories, large uncertainty
326 exists in RR of industrial boilers. Compared to the provincial inventory, ARs of ESP
327 and FGD were clearly underestimated in NJU and THU inventories (Table S5), hence
328 the TA in NJU was calculated 23% smaller than that in provincial inventory, leading to
329 a 747 kg increase in Hg emission estimate. In THU inventory, however, the much
330 higher RE of WET reduced the difference between national and provincial inventories,
331 and TA in THU inventory was only 2% smaller than the provincial one.

332 For CEM, both the provincial and THU inventories adopted the data from Yang
333 (2014), who measured provincial Hg contents in raw materials (limestone and other
334 raw materials) and Hg removal efficiency of DPT+DR in China. For AL , the
335 limestone consumption were calculated based on the clinker and cement production of
336 individual plants in the provincial inventory, while THU relied on cement production
337 at provincial level, leading to 13% smaller in AL and 1019 kg reduction in Hg
338 emission estimate. In addition, consumption of other raw materials for CEM were
339 ignored in THU inventory, leading to 1223 kg smaller in emission estimate compared
340 to the provincial inventory. According to on-site survey by Yang (2014), fly ash is
341 100% reused in DPT+DR, thus the technology minimizes the Hg removal by dust
342 collectors (ESP or FF). The AR of DPT+DR in THU was estimated at 82% at national
343 average level, while it reaches 89% in Jiangsu based on detailed provincial statistics
344 (CCA, 2011). Hence the TA employed in THU is 25% larger than that in provincial
345 inventory, resulting in 259 kg underestimation in Hg emissions. NJU and
346 AMAP/UNEP inventories failed to characterize the poor control of Hg from DPT+DR.
347 EFs applied in NJU came from early domestic measurements on rotary and shaft kiln
348 (Li, 2011; Zhang, 2007), ignoring the recent penetration of DPT+DR. In
349 AMAP/UNEP inventory, an effective Hg capture of 40% was generally assumed for
350 China's cement plants taking only the use of ESP and FF into account. The TA was
351 estimated 215% larger than that in the provincial inventory, resulting in 2253 kg
352 reduction in Hg emission estimate. EDGAR applied uniform emission factor (UEF) of



353 0.065g/t-clinker from EEA (2009), 32% lower than the average *EF* in the provincial
354 inventory. BNU developed S-shaped curves to estimate the time-varying dynamic
355 emission factors for non-coal combustion sector, based on the assumption of a
356 gradually declining trend in *EFs* along with increased controls of APCDs. As
357 mentioned above, however, the trend was not suitable for CEM due to the penetration
358 of DPT+DR. Thus UEF of 0.02 g/t cement estimated in BNU might result in
359 underestimation in Hg emissions, e.g., 7261 kg smaller than our provincial inventory.

360 For ISP, difficulty exists in emission estimation due to various Hg input sources
361 and complex production processes, and there is no consistent method in multi-scale
362 inventories so far. It was found that raw material production (limestone and dolomite),
363 coking, sintering and pig iron smelting with blast furnace account for most Hg
364 emissions in typical ISP in China (Wang et al., 2016). In our study, 11 factories
365 containing those processes are collected in PSC, and the emissions factors of 0.043
366 and 0.068 g/t-crude steel from Wang et al. (2016) are applied to plants with and
367 without raw material production, respectively. In other inventories, very few results
368 from domestic measurements were applied for Hg emission estimation for ISP in
369 China. NJU inventory took only coal combustion into account, and thus
370 underestimated the emissions for the sector by neglecting the Hg input along with iron
371 ore, limestone and other raw materials. THU inventory applied the emission factor of
372 0.04 g/t from Pacyna et al. (2010) for crude steel production. Besides difference in
373 emission factors, THU did not count the pig iron production in AL estimation, thus AL
374 in THU inventory is 29% lower than that in the provincial inventory, resulting in 1615
375 kg reduction in Hg emission estimate. Average *EF* in AMAP/UNEP was estimated at
376 0.039 g/t-pig iron by combining the input factor (0.05g/t-pig iron) calculated with a
377 mass balance method (UNEP, 2011a; BREF, 2012), and the removal effects of APCDs.
378 For comparison, *EF* used in our provincial inventory was recalculated at 0.064 g/t-pig
379 iron based on the hot metal charging ratio (*R* in Eq. (5); BREF, 2012). Lower *EF* in
380 AMAP/UNEP can partly be attributed to the overestimated *AR* of APCDs in ISP
381 without considering the gradual penetration of dust recycling as in CEM.

382 In general, the detailed activity and technology information including
383 manufacturing procedures and APCDs were investigated for individual plants in our
384 provincial inventory to improve the emission estimation, in contrast to previous
385 inventories that applied simplified or regional-average data. However, some crucial
386 parameters, e.g., Hg contents in coal and limestone, and Hg removal efficiencies of



387 APCDs, are still unavailable at plant level due to lack of measurements. Such
388 limitation thus indicates the necessity of more efforts on plant-specific emission
389 factors, and also motivates the uncertainty analysis for the provincial inventory, as
390 presented in Section 3.4.

391 **3.1.3 Comparisons of emissions for Categories 2 and 3**

392 For Categories 2 and 3, differences also exist in *EF* and *AL* between inventories.
393 For example, an emission factor of 0.22 g/t-waste combusted for MSWI based on
394 domestic tests (L. Chen et al., 2013; Hu et al., 2012) is applied in the provincial
395 inventory, while THU inventory applied 0.5 g/t from UNEP (2005), resulting in a
396 difference of 1024 kg in emission estimate. For primary Cu production, the provincial
397 inventory applied the emission factor of 0.4g/t-Cu from Wu et al. (2012), who
398 incorporated the results of available field measurements and the penetrations of
399 different smelting processes in China. BNU inventory, however, applied a much
400 higher emission factor at 8.9 g/t-Cu estimated by using an S-shaped curve based on
401 international results (Habashi, 1978; Nriagu, 1979; Pacyna, 1984; Pacyna and Pacyna,
402 2001; Streets et al., 2011; EEA, 2013). In NJU inventory, the emissions from NMS
403 and IUS were estimated much higher than the provincial inventory, attributed largely
404 to the different sources of activity data. For NMS, activity levels in NJU and
405 provincial inventories study were obtained from NSB (2011c) and NMIA (2011),
406 respectively. While NMIA (2011) provides the information on the production of
407 primary nonferrous metal (the major source of Hg emissions for NMS), the secondary
408 production were included in NSB (2011c), leading to possible overestimate in AL and
409 thereby Hg emissions. For IUS, provincial Hg consumption was allocated from the
410 national total use weighted by GDP in NJU inventory, while the data are directly
411 derived for Jiangsu from internal industrial report in the provincial inventory. In the
412 global inventories, moreover, all the emissions for Categories 2 and 3 in Jiangsu were
413 downscaled from national estimations attributed to lack of provincial information, and
414 big bias could be generated. For example, the large discrepancy for intentional use
415 and product waste associated sources between downscaled global and provincial
416 inventories is likely attributed to the overestimation in emissions from artisanal and
417 small-scale gold mining (ASGM) by global inventory (not included in Table 1 as no
418 ASGM was found by local source investigation).

419



420 **3.2 Hg speciation analysis of multi-scale inventories**

421 Besides the total emissions, Hg speciation has a significant impact on the
422 distance of Hg transport and chemical behaviors. Table 2 summarizes the mass
423 fractions of Hg species in emissions by sector for multi-scale inventories.

424 In general, as shown in Table 2, reduced Hg^0 but enhanced Hg^{2+} is estimated as
425 the spatial scale gets smaller. This can be mainly explained by the use of domestic
426 measurement results on Hg speciation for CEM, ISP and MSWI in the provincial
427 inventory. For CEM, the Hg^{2+} mass fraction for the dominating DPT+DR technology
428 tends to reach 75% based on available measurements (Yang, 2014), leading to a much
429 larger fraction of Hg^{2+} emissions in the provincial inventory. In contrast, speciated Hg
430 emissions were calculated using the same speciation profiles as those for coal
431 combustion in NJU inventory or the uniform profile ignoring the effects of APCDs in
432 AMAP/UNEP inventory. For ISP, heterogeneous Hg oxidation can be enhanced by the
433 high concentration of dust and existence of Fe_2O_3 in the flue gas during sintering
434 process, leading to large Hg^{2+} fraction for the sector reaching 66% (Wang et al., 2016).
435 For MSWI, results of domestic measurements (L. Chen et al., 2013; Hu et al., 2012)
436 were applied in the provincial and NJU inventories, elevating the Hg^{2+} fraction
437 compared to THU and AMAP/UNEP inventories that applied a global uniform
438 speciation profile without consideration of regional difference. It should be noted,
439 however, that uncertainty exists in the estimation of speciated emissions at small
440 spatial scale, attributed mainly to the limited samples in domestic measurements on
441 CEM and ISP.

442 As mentioned above, the “universal” profiles were applied for many sectors in
443 AMAP/UNEP inventory, ignoring the effects of various types of APCDs on Hg
444 speciation, particularly for coal combustion. However, the fate of Hg released to
445 atmosphere can primarily be affected by the removal mechanisms of APCDs. As
446 shown in Table 3, for example, Hg^0 mass fractions for ESP+FGD and FF+FGD tend
447 to be high reaching 83% and 78%, respectively, attributed to the relatively strong
448 removal effects of APCDs on Hg^{2+} and Hg^p . Once SCR is applied, an increase of Hg^{2+}
449 fraction can be observed, as the catalyst in SCR system can accelerate the conversion
450 of Hg^0 to Hg^{2+} (Wang et al., 2010). In addition, Hg^0 can also be oxidized to Hg^{2+} in FF
451 attributed to specific chemical composition in flue gas (chlorine, for example) and
452 high temperature (Wang et al., 2008; He et al., 2012). In contrast to global inventories,
453 therefore, national and provincial inventories take the effects of different APCDs into



454 account. Summarized in Table 3, considerable differences exist in the speciation
455 profiles for typical APCDs between national and provincial inventories, attributed
456 mainly to the various data used from domestic field measurements. Excluding the
457 measurement results on WET (Zhang et al., 2012), for example, NJU inventory
458 assumed the species profile from WET to be the same as CYC, and thereby largely
459 underestimated the mass fraction of Hg^0 for OIB where WET is widely applied.
460 Besides, the penetrations of APCDs are also crucial in determination of speciated Hg
461 emissions. As indicated in Table 3, with similar speciation profiles for FGD applied
462 between multi-scale inventories, the difference in Hg speciation is relatively small for
463 CPP between inventories, given the relatively accurate and transparent information on
464 FGD penetration in CPP used in all the inventories. For OIB, however, the difference
465 in Hg speciation is significantly elevated, as large diversity in APCDs penetration is
466 found between multi-scale inventories, as shown in Table S5. With the penetration of
467 FF and ESP highly underestimated, for example, THU provided a lower estimation in
468 Hg^{2+} fraction compared to other inventories.

469

470 **3.3 Comparisons of spatial patterns of emissions between multi-scale inventories**

471 Figure 3 presents the spatial distributions of total and speciated Hg emissions in
472 Jiangsu province at $0.05^\circ \times 0.05^\circ$. Similar patterns are found between species.
473 Relatively high emissions are distributed over northwestern and southern Jiangsu,
474 resulting from intensive coal combustion, and cement and iron & steel production, as
475 indicated in Figure S1 in the supplement. As an important energy base, Xuzhou in
476 northwestern Jiangsu contains a large number of coal combustion sources, while great
477 energy demand exists in southern Jiangsu attributed to highly developed economy.
478 The gross industrial production of the five cities in southern Jiangsu (Nanjing,
479 Zhenjiang, Suzhou, Wuxi and Changzhou) in 2010 accounted for 64% of the total
480 amount in the province. For cement production, as an example, the clinker
481 manufacture plants that dominate the Hg emissions compared to the subsequent
482 mixing stage (UNEP, 2011a), are mainly located in southern Jiangsu, depending on
483 the distribution of limestone resources.

484 In order to compare the spatial distribution of provincial inventory to that of NJU,
485 THU, AMAP/UNEP and EDGARv4.tox2 inventories, we upscale the gridded
486 provincial emissions from $0.05^\circ \times 0.05^\circ$ to the resolutions of $0.125^\circ \times 0.125^\circ$, $36 \times 36 \text{ km}$,
487 $0.5^\circ \times 0.5^\circ$ and $0.1^\circ \times 0.1^\circ$ respectively. Differences in gridded Hg^T emissions for



488 Jiangsu between the upscaled provincial inventory and other multi-scale inventories
489 are presented in Figure 4. Although selected sources were identified as point sources
490 in global/national inventories, e.g., CEM in NJU and THU, ISP in EDGARv4.tox2,
491 and CPP in all the inventories, the emission fraction of point sources (Categories 1
492 and 2) is significantly elevated to 92% in the provincial inventory. In particular, the
493 emissions from point sources of which the geographic information were corrected
494 account for 78% of total emissions in the province.

495 As illustrated in Figure 4, differences in gridded emissions between provincial
496 and other inventories NJU, THU, AMAP/UNEP and EDGARv4.tox2 are respectively
497 in the ranges of -760~+4135 kg, -1429~+3217 kg, -1424~+3043 kg and -1078~+3895
498 kg. Grids with differences more than 400 kg/yr are commonly distributed in southern
499 and northwestern Jiangsu, and coincide well with the locations of point sources that
500 are estimated to have relatively large emissions in the provincial inventory. It can thus
501 be indicated that differences in spatial patterns of Hg emissions come mainly from the
502 inconsistent information of big point sources between the provincial inventory and
503 national/global inventories. For CPP, AMAP/UNEP obtained information of identified
504 facilities from Wikipedia
505 (http://en.wikipedia.org/wiki/List_of_power_stations_in_Asia), and failed to include a
506 number of coal-fired power plants built in recent years (Steenhuisen et al., 2015). For
507 EDGARv4.tox2, proxy data (e.g., electricity production) from Carbon Monitoring
508 Action (CARMA, <http://carma.org/blog/carma-notes-future-data/>) are used to allocate
509 Hg emissions. Although CARMA incorporates all the major disclosure databases,
510 uncertainties still exist in certain individual plants attributed to lack of information on
511 geographical locations and control technologies. Moreover, as the most updated
512 information in CARMA was collected in 2009, EDGAR had to predict the emissions
513 of CPP for 2010, and thus could not fully track the actual changes in the sector, e.g.,
514 operation of new-built units, or shutting down the small ones. Similarly, NJU and
515 THU obtained the information of power units from a relatively old database (Zhao et
516 al., 2008), and made further assumptions on activities and penetrations of APCDs to
517 update the emissions of individual plants. As a result, in general, larger emissions are
518 found in the provincial inventory than other inventories in southern Jiangsu where big
519 power plants are located, particularly in Nanjing and northern Suzhou. As detailed
520 information at plant level is unavailable for each inventory, we speculate the
521 discrepancy resulted mainly from the underestimation (or missing) in coal



522 consumption in previous electric power generation databases that other inventories
523 relied on, and the use of regional/national-average information on APCD penetration
524 by certain inventories (e.g., THU and AMAP/UNEP). The comparison in
525 northwestern Jiangsu is less conclusive: the emissions in the areas with big power
526 plants were estimated lower in provincial inventory than AMAP/UNEP (Figure 4(c)).
527 Such difference, however, result not only from the varied estimations in CPP
528 emissions but also from discrepancy in other sources, e.g., intensive emissions from
529 industrial sources in the area in AMAP/UNEP. For ISP and CEM, similarly, higher
530 emissions were estimated by the provincial inventory for areas with big plants in
531 Zhenjiang, Suzhou and Changzhou in southern Jiangsu. In the provincial inventory, as
532 described in Section 2, the activities for each manufacturing processes were
533 investigated for individual plants and the information is taken into consideration in
534 emission estimation. In contrast, the emissions were allocated based only on the
535 production of individual plants in national inventories (THU and NJU), thus the
536 effects of manufacturing technologies on emissions were ignored. Moreover, some
537 CEM and ISP plants were missed in those national inventories, leading to
538 underestimation in emissions for corresponding regions. In general, due to lack of
539 plant-specific information, previous inventories failed to capture the relatively large
540 emissions from big point sources. When the national inventory was applied in CTM,
541 the simulated concentrations of Hg^{T} were usually lower than the observation at rural
542 sites in eastern China (Wang et al., 2014). Since many big plants are commonly being
543 moved from urban to rural areas (Zhao et al., 2015b; Zhou et al., in preparation),
544 improvement in model performance could be expected when the elevated emissions in
545 rural areas are estimated and used for CTM, incorporating the accurate information of
546 individual big plants.

547 With much fewer big emitters, discrepancies in gridded emissions for other part
548 of Jiangsu resulted largely from the allocation of considerable emissions as area
549 sources in national and global inventories. For example, in spite of an estimation of
550 8496 kg smaller than the provincial inventory in total emissions, NJU inventory
551 applied proxies (e.g., population and GDP) to allocate the emissions except those
552 from CPP, resulting in higher emissions in central and most part of northern Jiangsu
553 (Figure 4(a)). Similar patterns are also found for THU (Figure 4(b)) and
554 AMAP/UNEP (Figure 4(c)) compared to provincial inventory.

555 Besides the total emissions, differences in spatial distribution of speciated Hg



556 emissions between multi-scale inventories are presented in Figure S3 in the
557 supplement. The various patterns for species are largely influenced by the distribution
558 of different types of big point sources, as the speciation profiles vary significantly
559 between source types in the national and provincial inventories (Table 2). Compared
560 to other inventories, larger Hg^0 emissions were found in the provincial inventory in
561 southern Jiangsu (particularly Zhenjiang and Taizhou) where CPPs that have large
562 fraction of Hg^0 are intensively located. Elevated Hg^{2+} emissions were dominated by
563 intensive CEM industry in Changzhou, Wuxi and Zhenjiang in southern Jiangsu, as
564 the Hg^{2+} fraction of CEM reaches 73% in the provincial inventory. In contrast to Hg^0
565 and Hg^{2+} , differences in Hg^{p} emissions between inventories in central Jiangsu are
566 closely related with the locations of OIB plants, attributed mainly to the relatively
567 poor understanding of the particle control and thereby Hg^{p} release of OIB. The
568 emissions in the provincial inventory is larger than THU but smaller than
569 AMAP/UNEP, as the Hg^{p} mass fraction of OIB was assumed at 2% in THU while it
570 reached 10% in AMAP/UNEP (Table 2).

571 The vertical distribution of Hg releases, which is crucial for the transport range
572 of atmospheric Hg, is also analyzed in this work. Four groups of release height are
573 defined: 0-58m, 58-141m, 141-250m and >250m. Based on the detailed information
574 of emission sources, the fractions of Hg releases into the four groups for CPP are 2%,
575 66%, 31%, and 1%, respectively, and the analogue numbers for OIB, ISP, and CEM
576 are 85%, 13%, 2%, and 0%; 4%, 44%, 12%, and 4%; and 6%, 94%, 0%, and 0%,
577 respectively. The release heights for rest sources are uniformly assumed at the range
578 of 0-58m. As a result, the fractions of total Hg emissions in the four groups are
579 estimated as 35%, 53%, 11% and 1%. In AMAP/UNEP inventory, as a comparison,
580 the fractions at the height of 0-50m, 50-150m and >150m were estimated at 23%,
581 53% and 24% respectively, with larger share in Hg emitted over 150m than that in our
582 provincial inventory.

583

584 3.4 Uncertainty of the provincial inventory

585 As summarized in Table 4, the uncertainties of speciated Hg emissions in the
586 provincial inventory are estimated at -24%~+82% (95% confidence intervals (CI)
587 around central estimates), -34%~+99%, -23%~+68%, and -34%~+270% for Hg^{T} , Hg^0 ,
588 Hg^{2+} and Hg^{p} , respectively. For comparison, the uncertainties of Jiangsu emissions
589 from major sectors including CPP, CEM, ISP and OIB in NJU inventory are



590 recalculated following Zhao et al. (2015a) and provided in Table 4 as well. As can be
591 seen, the uncertainties for major sources in the provincial inventory were smaller than
592 those in NJU inventory, attributed largely to the bottom-up approach used in
593 provincial inventory with more accurate information on activity levels and APCDs
594 applications for individual plants of Category 1. In addition, with more field
595 measurements on Hg contents in coal and limestone incorporated, the uncertainties of
596 HgC_{raw} and $HgC_{Limestone}$ are significantly reduced, resulting from the mechanism of
597 error compensation when HgC_{raw} of coals produced in different provinces are taken
598 into account in the inter-provincial flow model for coal transport, and the successful
599 application of bootstrap simulation, respectively. As a result, the uncertainties of
600 emissions from CPP, OIB and CEM are effectively reduced in the provincial
601 inventory.

602 The parameters contributing most to uncertainties and their contributions to the
603 variance of corresponding emission estimates are summarized by sector in Table S8 in
604 the supplement. For CPP and OIB, parameters related to emission factors contribute
605 most to the uncertainties of Hg^T emissions, including the HgC_{raw} in provinces with
606 largest contribution to the input of coal consumed in Jiangsu (i.e., Shaanxi and Inner
607 Mongolia), and the removal efficiencies (RE) or release ratios (RR) of Hg for typical
608 APCD (ESP+FGD) and combustor type (grate boiler). HgC_{raw} of coals produced in
609 Shaanxi and Inner Mongolia that collectively accounted for 34% of coal consumption
610 in Jiangsu, contributed 26% and 18% to the uncertainties of Hg emissions for CPP,
611 and 15% and 11% to those for OIB, respectively. It is thus essential to conduct
612 systematic and synergetic measurements on HgC_{raw} in different regions (particularly
613 those with large coal production) to constrain the uncertainties of Hg emission
614 estimation for coal combustion sources, at both regional and national scales. Given
615 the wide application of ESP+FGD in CPP (70% in coal consumption), $RE_{ESP+FGD}$ is
616 estimated to contribute 20% to Hg emissions from CPP. Local measurements on RE of
617 typical APCDs, which have started in Jiangsu (JSEMC, 2013; Xie and Yi, 2014), are
618 expected to potentially improve the Hg emission estimation at regional level.
619 Although applied in 92% of OIB plants in Jiangsu, there are very few studies on Hg
620 release rate of grate boiler, resulting in a contribution of 5% to the emission
621 uncertainty. For CEM, $HgC_{Limestone}$ dominates the uncertainties of Hg emissions, with
622 the contribution estimated at 84%. Attributed to lack of detailed information,
623 provincial average of $HgC_{Limestone}$ with the lognormal distribution fitted through



624 bootstrap simulation based on available measurements (Figure S2 and Table S6) was
625 uniformly applied for all the individual plants, leading to the enhanced contribution to
626 the uncertainty. For ISP, *EF* of limestone and dolomite production contributes 60% to
627 Hg emissions, as the process is estimated to account for 88% of emissions from the
628 entire sector. In addition, *AL* from the biggest ISP factory, which accounted for 40%
629 and 75% of pig iron and crude steel production for the whole province, respectively,
630 contributes 24% to the total uncertainty of ISP sector. The result indicates a necessity
631 of specific investigation on super emitters. For rest sources, MSWI, BIO and O&G are
632 the biggest sources for Hg^T emissions, and *EFs* of those types of sources thus
633 contribute most to the emission uncertainty.

634 In most cases, parameters with big contribution to uncertainty of Hg^T also play
635 crucial roles in uncertainty of speciated emissions. Moreover, the speciation profiles
636 for typical source types and APCDs are identified as key parameters to the
637 uncertainties of speciated emissions as well. For example, the mass fraction of Hg²⁺
638 from ESP+FGD, and that of Hg^P from ESP are the biggest contributors to
639 uncertainties of Hg²⁺ and Hg^P emissions from CPP, respectively. For OIB, the mass
640 fraction of Hg^P from sources without any control is much higher than those with
641 APCDs (Table 3), thus it plays an important role in the emission uncertainty, with the
642 contribution estimated at 35%. For CEM and ISP, studies on speciation profiles are
643 limited so far, and the speciation profiles for DPT+DR and ISP plants contribute
644 largely to uncertainties of speciated emissions.

645

646 4 CONCLUSIONS

647 Taking Jiangsu province in China as an example, the discrepancies and their
648 sources of atmospheric Hg emission estimations in multi-scale inventories applying
649 varied methods and data are thoroughly analyzed. Using a bottom-up approach that
650 integrates best available information of individual plants and most recent field
651 measurements, the total Hg emissions in Jiangsu 2010 are calculated at 39 105 kg, and
652 the estimate is larger than any other national/global inventories. CPP, ISP, CEM and
653 OIB collectively accounted for 90% of the total emissions. Comparisons between
654 available studies demonstrate that the information gaps of multi-scale inventories lead
655 to big differences in Hg emission estimation. Discrepancies in emissions between
656 inventories for the above-mentioned major sources come primarily from various data



657 sources for activity levels, Hg contents in coals and total abatement effects of APCDs.
658 Notable increase in Hg²⁺ emissions is estimated with the bottom-up approach
659 compared to other global/national inventories, attributed mainly to the adoption of
660 domestic measurement results with elevated mass fraction of Hg²⁺ for CEM, ISP and
661 MSWI. Inconsistent information of big point sources lead to large differences in
662 spatial distribution of emissions between provincial and other inventories, particularly
663 in southern and northwestern of the province where intensive coal combustion and
664 industry are located. Improved estimates in emission level, speciation and spatial
665 distribution are expected to better support the regional chemistry transport modeling
666 of atmospheric Hg. Compared to the national inventory, uncertainties of Hg emissions
667 are reduced in provincial inventory using the bottom-up approach. Extensive and
668 dedicated measurements are urgently suggested on Hg contents in coal/limestone and
669 removal efficiency of dominating APCDs to further improve the emission estimation
670 at regional/local scales.

671

672

ACKNOWLEDGEMENT

673 This work was sponsored by the Natural Science Foundation of China
674 (41575142), Natural Science Foundation of Jiangsu (BK20140020), Jiangsu Science
675 and Technology Support Program (SBE2014070918), and Special Research Program
676 of Environmental Protection for Commonweal (201509004). We would like to
677 acknowledge Hezhong Tian from Beijing Normal University and Simon Wilson from
678 UNEP/AMAP Expert Group for the detailed information on national/global Hg
679 emission inventories.

680

681

REFERENCES

- 682 AMAP/UNEP: Technical Background Report to the Global Atmospheric Mercury
683 Assessment, Arctic Monitoring and Assessment Programme, Oslo, Norway/UNEP
684 Chemicals Branch, Geneva, Switzerland, 159 pp., 2008.
685 AMAP/UNEP: Technical Background Report for the Global Mercury Assessment,
686 Arctic Monitoring and Assessment Programme, Oslo, Norway/UNEP Chemicals
687 Branch, Geneva, Switzerland, 263 pp., 2013.
688 Best Available Techniques Reference Document (BREF) for Iron and Steel Production,



- 689 Industrial Emissions Directive 2010/75/EU. (Integrated Pollution Prevention and
690 Control), European Commission, March, 2012, online at:
691 http://eippcb.jrc.ec.europa.eu/reference/BREF/IS_Adopted_03_2012.pdf.
- 692 Chen, C., Wang, H. H., Zhang, W., Hu, D., Chen, L., Wang, X. J.: High-resolution
693 inventory of mercury emissions from biomass burning in China for 2000-2010 and a
694 projection for 2020, *J. Geophys. Res.*, 118, 12248-12256, 2013.
- 695 Chen, L., Liu, M., Fan, R., Ma, S., Xu, Z., Ren, M., He, Q.: Mercury speciation and
696 emission from municipal solid waste incinerators in the Pearl River Delta, South
697 China, *Sci. Total Environ.*, 447, 396–402, 2013.
- 698 China Cement Association (CCA) : China cement almanac, China Building Industry
699 Press, 2011.
- 700 Fu, X. W., Feng, X. B., Sommar, J., Wang, S. F.: A review of studies on atmospheric
701 mercury in China, *Sci. Total Environ.*, 421–422, 73–81, 2012.
- 702 Fu, X. W., Zhang, H., Lin, C. J., Feng, X. B., Zhou, L. X., Fang, S. X.: Correlation
703 slopes of GEM / CO, GEM / CO₂, and GEM / CH₄ and estimated mercury emissions
704 in China, South Asia, the Indochinese Peninsula, and Central Asia derived from
705 observations in northwestern and southwestern China, *Atmos. Chem. Phys.*, 15,
706 1013–1028, 2015.
- 707 European Environment Agency (EEA): EMEP/EEA air pollutant emission inventory
708 guidebook 2009, Technical report No 9/2009, available online at:
709 <http://www.eea.europa.eu/publications/emep-eea-emission-inventory-guidebook-2009>
- 710 European Environment Agency (EEA): EMEP/EEA air pollutant emission inventory
711 guidebook 2013, available online at:
712 <http://www.eea.europa.eu/publications/emep-eea-guidebook-2013>
- 713 Habashi, F.: Metallurgical plants: how mercury pollution is abated, *Environ. Sci.*
714 *Technol.*, 12, 1372-1376, 1978.
- 715 He, Z. Q., Kan, Z. N., Qi, L. M., Han, X. F.: Analysis to mercury removal
716 performance test of bag-type dust collector, *Inner Mongolia Electric Power*, 30 (1),
717 0040-0042, 2012 (in Chinese).
- 718 Hu, D., Zhang, W., Chen, L., Ou, L. B., Tong, Y. D., Wei, W., Long, W. J., Wang, X.
719 J.: Mercury emissions from waste combustion in China from 2004 to 2010, *Atmos.*
720 *Environ.*, 62, 359–366, 2012.
- 721 Jiangsu Environment Monitoring Center (JSEMC): Research on mercury emissions in



- 722 flue gas of coal-fired power plants in Jiangsu Province, Interim report, 2013 (in
723 Chinese).
- 724 Li, W.: Characterization of Atmospheric Mercury Emissions from Coal-fired Power
725 Plant and Cement Plant (Master Thesis), Xi'an University, Chongqing, China, 2011
726 (in Chinese).
- 727 Lin, C. J., Pan, L., Streets, D. G., Shetty, SK., Jang, C., Feng, X., Chu, H. W., Ho, T.
728 C.: Estimating mercury emission outflow from East Asia using CMAQ-Hg, Atmos.
729 Chem. Phys., 10(4), 1853-1864, 2010.
- 730 Muntean, M., Janssens-Maenhout, G., Song, S., Selin, N. E., Olivier, J. G. J.,
731 Guizzardi, D., Maas, R., Dentener, F.: Trend analysis from 1970 to 2008 and model
732 evaluation of EDGARv4 global gridded anthropogenic mercury emissions,
733 Sci. Total Environ., 494-495, 337-350, 2014.
- 734 Nriagu, J. O.: Global inventory of natural and anthropogenic emissions of trace metals
735 to the atmosphere, Nature, 279, 409-411, 1979.
- 736 National Statistical Bureau of China (NSB): China Statistical Yearbook, China
737 Statistics Press, Beijing, 2011a.
- 738 National Statistical Bureau of China (NSB): China Energy Statistical Yearbook, China
739 Statistics Press, Beijing, 2011b.
- 740 National Statistical Bureau of China (NSB): China Industry Economy Statistical
741 Yearbook, China Statistics Press, Beijing, 2011c.
- 742 Nonferrous Metal Industry Association of China (NMIA): Yearbook of Nonferrous
743 Metals Industry of China, China Statistics Press, Beijing, 2011.
- 744 Pacyna, E. G., Pacyna, J. M., Sundseth, K., Munthe, J., Kindbom, K., Wilson, S.,
745 Steenhuisen, F., Maxson, P.: Global emission of mercury to the atmosphere from
746 anthropogenic sources in 2005 and projections to 2020, Atmos. Environ., 44,
747 2487-2499, 2010.
- 748 Pacyna, J. M.: Estimation of the atmospheric emissions of trace elements from
749 anthropogenic sources in Europe, Atmos. Environ., 18, 41-50, 1984.
- 750 Pacyna, J. M., and Pacyna, E. G.: An assessment of global and regional emissions of
751 trace metals to the atmosphere from anthropogenic sources worldwide, Environ. Rev.,
752 9, 269-298, 2001.
- 753 Pirrone, N., Cinnirella, S., Feng, X., Finkelman, R. B., Friedli, H. R., Leaner, J.,



- 754 Mason, R., Mukherjee, A. B., Stracher, G. B., Streets, D. G., Telmer, K.: Global
755 mercury emissions to the atmosphere from anthropogenic and natural sources, Atmos.
756 Chem. Phys., 10, 5951-5964, 2010.
- 757 Pirrone, N., Mason, R. P. (Eds): Mercury fate and transport in the global atmosphere,
758 Springer US., 2009.
- 759 Steenhuisen, F., Wilson, S. J.: Identifying and characterizing major emission point
760 sources as a basis for geospatial distribution of mercury emissions inventories, Atmos.
761 Environ., 112, 167-177, 2015.
- 762 Streets, D. G., Devane, M. K., Lu, Z., Bond, T. C., Sunderland, E.M., and Jacob, D.J.:
763 All-time releases of mercury to the atmosphere from human activities, Environ. Sci.
764 Technol., 45, 10485–10491, 2011.
- 765 Tang, S. L., Feng, X. B., Shang, L. H., Yan, H. Y., Hou, Y. M.: Mercury speciation and
766 emissions in the flue gas of a small-scale coal-fired boiler in Guiyang, Research of
767 Environmental Sciences, 17, 74-76, 2004 (in Chinese).
- 768 Tian, H. Z., Liu, K. Y., Zhou, J. R., Lu, L., Hao, J. M., Q, P. P., G, J. J., Zhu, C. Y.,
769 Wang, K., Hua, S. B.: Atmospheric Emission Inventory of Hazardous Trace Elements
770 from Chinas Coal-Fired Power Plants Temporal Trends and Spatial Variation
771 Characteristics, Environ. Sci. Technol., 48, 3575-3582, 2014.
- 772 Tian, H. Z., Wang, Y., Xue, Z. G., Cheng, K., Qu, Y. P., Chai, F. H., Hao, J. M.: Trend
773 and characteristics of atmospheric emissions of Hg, As, and Se from coal combustion
774 in China, 1980–2007, Atmos. Chem. Phys., 10, 11905-11919, 2010.
- 775 Tian, H. Z., Zhu, C. Y., Gao, J. J., Cheng, K., Hao, J. M., Wang, K., Hua, S. B., Wang,
776 Y., Zhou, J. R.: Quantitative assessment of atmospheric emissions of toxic heavy
777 metals from anthropogenic sources in China: historical trend, spatial distribution,
778 uncertainties, and control policies, Atmos. Chem. Phys., 15, 10127-10147, 2015.
- 779 Timmermans, R. M. A., Denier van der Gon, H. A. C., Kuenen, J. J. P., Segers, A. J.,
780 Honoré, C., Perrussel, O., Builtjes, P. J. H., Schaap, M.: Quantification of the urban
781 air pollution increment and its dependency on the use of down-scaled and bottom-up
782 city emission inventories, Urban Climate, 6, 44-62, 2013.
- 783 United Nations Environment Programme (UNEP): Toolkit for Identification and
784 Quantification of Mercury Releases, UNEP Chemicals Branch, 2005.



- 785 United Nations Environment Programme (UNEP): Toolkit for Identification and
786 Quantification of Mercury Releases, Revised Inventory Level 2 Report including
787 Description of Mercury Source Characteristics, Version 1.1., January 2011, 2011a,
788 available online at:
789 [www.unep.org/hazardoussubstances/Portals/9/Mercury/Documents/Publications/Tool](http://www.unep.org/hazardoussubstances/Portals/9/Mercury/Documents/Publications/Toolkit/Hg%20Toolkit-Reference-Report-rev-Jan11.pdf)
790 [kit/Hg%20Toolkit-Reference-Report-rev-Jan11.pdf](http://www.unep.org/hazardoussubstances/Portals/9/Mercury/Documents/Publications/Toolkit/Hg%20Toolkit-Reference-Report-rev-Jan11.pdf).
- 791 United Nations Environment Programme (UNEP): Reducing Mercury Emissions from
792 Coal Combustion in the Energy Sector of China, Prepared for the Ministry of
793 Environment Protection of China and UNEP Chemicals, Tsinghua University, Beijing,
794 China, February 2011, 2011b, available online at:
795 [www.unep.org/hazardoussubstances/Portals/9/Mercury/Documents/coal/FINAL%20](http://www.unep.org/hazardoussubstances/Portals/9/Mercury/Documents/coal/FINAL%20Chinese%20Coal%20Report%20-%202011%20March%202011.pdf)
796 [hinese Coal%20Report%20-%202011%20March%202011.pdf](http://www.unep.org/hazardoussubstances/Portals/9/Mercury/Documents/coal/FINAL%20Chinese%20Coal%20Report%20-%202011%20March%202011.pdf).
- 797 US Environmental Protection Agency (EPA): US National Emission Inventory 2008
798 version 2 (April 2012), 2012, available online at:
799 www.epa.gov/ttn/chief/net/2008inventory.htm.
- 800 US Geological Survey (USGS): Mercury content in coal mines in China (unpublished
801 data), 2004.
- 802 Wang, Q. C., Shen, W. G., Ma, Z. W.: Estimation of Mercury Emission from Coal
803 Combustion in China, Environ. Sci. Technol., 34, 2711-2713, 2000.
- 804 Wang, L., Wang, S. X., Zhang, L., Wang, Y. X., Zhang, Y. X., Nielsen, C., McElroy,
805 M. B., Hao, J. M.: Source apportionment of atmospheric mercury pollution in China
806 using the GEOS-Chem model, Environ. Pollut., 190(7), 166-175, 2014.
- 807 Wang, S. X., Zhang, L., Li, G. H., Wu, Y., Hao, J. M., Pirrone, N., Sprovieri, F.,
808 Ancora, M. P.: Mercury emission and speciation of coal-fired power plants in China,
809 Atmos. Chem. Phys., 10, 1183-1192, 2010.
- 810 Wang, Y. J., Duan, Y. F., Yang, L. G., Jiang, Y. M., Wu, C. J., Wang, Q., Yang, X. H.:
811 Analysis of the factors exercising an influence on the morphological transformation of
812 mercury in the flue gas of a 600MW coal-fired power plant,
813 Journal of Engineering for Thermal Energy and Power, 04, 399-403, 2008 (in
814 Chinese).
- 815 Wang, F. Y., Wang S. X., Zhang, L., Yang, H., Gao, W., Wu, Q. R., Hao, J. M.:
816 Mercury mass flow in iron and steel production process and its implications for
817 mercury emission control, Journal of Environmental Sciences, 2016 (in press),



- 818 available online at: <http://dx.doi.org/10.1016/j.jes.2015.07.019>.
- 819 Wu, Q. R., Wang, S. X., Zhang, L., Song, J. X., Yang, H., Meng, Y.: Update of
820 mercury emissions from China's primary zinc, lead and copper smelters, 2000–2010,
821 Atmos. Chem. Phys., 12, 11153-11163, 2012.
- 822 Xie, X., Yin, W.: Nanjing Thermal Power Plant Boiler Flue Gas Mercury Emissions in
823 the Survey, Environmental Monitoring and Forewarning, 6, 47-49, 2014.
- 824 Yang, H.: Study on atmospheric mercury emission and control strategies from cement
825 production in China, M.S. thesis, Tsinghua University, Beijing, China, 2014 (in
826 Chinese).
- 827 Yao, W., Qu, X. H., Li, H. X., Fu, Y. F.: Production, collection and treatment of
828 garbage in rural areas in China, Journal of Environment and Health, 26, 10-12, 2009
829 (in Chinese).
- 830 Zhang, L.: Emission Characteristics and Synergistic Control Strategies of
831 Atmospheric Mercury from Coal Combustion in China, Ph. D thesis, Tsinghua
832 University, Beijing, China, 2012 (in Chinese).
- 833 Zhang, L.: Research on mercury emission measurement and estimate from
834 combustion resources (Master Thesis), Zhejiang University, Hangzhou, China, 2007
835 (in Chinese).
- 836 Zhang, L., Wang, S. X., Meng, Y., Hao, J. M.: Influence of mercury and chlorine
837 content of coal on mercury emissions from coal-fired power plants in China, Environ.
838 Sci. Technol., 46, 6385-6392, 2012.
- 839 Zhang, L., Wang, S. X., Wang, L., Wu, Y., Duan, L., Wu, Q. R., Wang, F. Y., Yang, M.,
840 Yang, H., Hao, J. M., Liu, X.: Updated Emission Inventories for Speciated
841 Atmospheric Mercury from Anthropogenic Sources in China, Environ. Sci. Technol,
842 49, 3185–3194, 2015.
- 843 Zhao, Y., Wang, S. X., Duan, L., Lei, Y., Cao, P. F., Hao, J. M.: Primary air pollutant
844 emissions of coal-fired power plants in China: current status and future prediction,
845 Atmos. Environ., 42, 8442-8452, 2008.
- 846 Zhao, Y., Nielsen, C. P., Lei, Y., McElroy, M. B., Hao, J. M.: Quantifying the
847 uncertainties of a bottom-up emission inventory of anthropogenic atmospheric
848 pollutants in China, Atmos. Chem. Phys., 11, 2295-2308, 2011.



849 Zhao, Y., Nielsen, C. P., McElroy, M. B., Zhang, L., Zhang, J.: CO emissions in
850 China: uncertainties and implications of improved energy efficiency and emission
851 control, *Atmos. Environ.*, 49, 103-113, 2012.

852 Zhao, Y., Zhong, H., Zhang, J., Nielsen, C. P.: Evaluating the effects of China's
853 pollution controls on inter-annual trends and uncertainties of atmospheric mercury
854 emissions, *Atmos. Chem. Phys.*, 15, 4317-4337, 2015a.

855 Zhao, Y., Qiu, L. P., Xu, R. Y., Xie, F. J., Zhang, Q., Yu, Y. Y., Nielsen, C. P., Qin,
856 H. X., Wang, H. K., Wu, X. C., Li, W. Q., Zhang, J.: Advantages of a city-scale
857 emission inventory for urban air quality research and policy: the case of Nanjing, a
858 typical industrial city in the Yangtze River Delta, China, *Atmos. Chem. Phys.*, 15,
859 18691-18746, 2015b.

860 Zhou, Y., Zhao, Y., Mao, P., Zhang, Q., Zhang, J., Qiu, L., Yang, Y.: Development of
861 a high-resolution emission inventory and its evaluation through air quality modeling
862 for Jiangsu Province, China, 2016 (in preparation).

863 Zhu, J., Wang, T. J., Bieser, J., Matthias, V.: Source attribution and process analysis
864 for atmospheric mercury in East China simulated by CMAQ-Hg, *Atmos. Chem. Phys.*,
865 15, 8767-8779, 2015.

866

867



TABLES

Table 1 Emission estimates for Jiangsu in 2010 and species from multi-scale inventories by sector. Recall from Section 2 the abbreviations for emission sources: CPP: coal-fired power plants; RCC: residential coal combustion; O&G: oil and gas combustion; OIB: other industrial coal combustion; CEM: cement production; ISP: iron & steel plants; NMS: nonferrous metal smelting; AP: aluminum production; LGM: large-scale gold mining; MM: mercury mining; HC: human cremation; MSWI: municipal solid waste incineration; RSWI: rural solid waste incineration; BFLP: battery/fluorescent lamp production; BIO: biofuel use/biomass open burning; and PVC: PVC production.

	CPP ¹	RCC ³	O&G ³	OIB ¹	CEM ¹	ISP ¹	NMS ²	AP ²	LGM	MM	HC ³	MSWI ²	RSWI ³	BFLP ²	BIO ³	PVC ²	Total
Hg ¹																	
Bottom-up	11549	195	930	8652	9264	5654	91	29	0	0	326	1009	365	158	461	423	39106
NJU	11208	165	930	6901	1137	2243	2158	/	23	51	/	1009	457	1225	500	2603	30610
THU	10768	345	752	10680	8238	2539	0	29	0	0	326	2294	244	244	219	/	36434
BNU	12883	267	898	10172	3288	2669	2022	6	/	/	/	308	4976 ^c	303	303	/	32816
AMAP/UNEP		9292 ^a					17759 ^b										32027
EDGARv4.tox2	10233 ^d	1181 ^e	/	3310 ^f	6364	447	413	/	/	/	1017	1017	/	/	43	/	23008
Hg ⁰																	
Bottom-up	8811	91	465	4689	2461	1908	45	23	0	0	313	1017	47	158	350	423	20801
NJU	8133	42	465	2042	685	1208	1189	/	16	41	/	190	980	980	380	2082	17453
THU	7689	247	376	6995	2793	863	0	23	0	0	313	2202	244	244	162	/	21907
AMAP/UNEP		4646 ^a					14207 ^b						4668 ^c				23521
Hg ²⁺																	
Bottom-up	2653	73	372	3394	6752	3746	45	4	0	0	0	868	314	0	23	0	18244
NJU	2900	45	372	4003	431	835	963	/	7	8	/	868	59	184	25	390	11090
THU	3058	92	301	3471	5338	1676	0	4	0	0	0	0	0	0	11	/	13951
AMAP/UNEP		3717 ^a					2707 ^b						238 ^c				6662
Hg ^p																	
Bottom-up	85	32	93	569	51	0	0	1	0	0	13	10	4	0	88	0	946
NJU	175	79	93	855	20	200	6	/	0	3	/	10	5	61	95	130	1732
THU	22	6	75	214	107	0	0	1	0	0	13	92	70 ^c	0	46	/	576
AMAP/UNEP		929 ^a					845 ^b										1844

^{1,2,3} Sectors in category 1, 2 and 3 as classified in Section 2. ^a Stationary combustion sources: power plants, distributed heating, and other energy use (industrial sources excluded). ^b Industrial sources including stationary combustion for industry, CEM, ISP, NMS, AP, LGM and MM. ^c Intentional use and product waste associated sources: artisanal and small-scale gold mining, solid waste incineration and other product waste disposal, chlor-alkali industry, and human cremations. ^{d, e, f} Both coal and other fossil fuel combustion included.



Table 2 Hg speciation profiles by sector and the mass fractions to total emissions in multi-scale inventories (%).

Sector	Provincial inventory			NJU			THU			AMAP/UNEP		
	Hg ⁰	Hg ²⁺	Hg ^p	Hg ⁰	Hg ²⁺	Hg ^p	Hg ⁰	Hg ²⁺	Hg ^p	Hg ⁰	Hg ²⁺	Hg ^p
CPP	76	23	1	73	26	2	71	28	0	50	40	10
RCC	46	37	16	25	27	48	71	27	2	50	40	10
O&G	50	40	10	50	40	10	50	40	10	50	40	10
OIB	54	39	7	30	57	13	66	33	2	50	40	10
CEM	27	73	1	60	38	2	34	65	1	80	15	5
ISP	34	66	0	54	37	9	34	66	0	80	15	5
NMS	50	50	0	55	45	0		/		80	15	5
AP	80	15	5		/		80	15	5	80	15	5
LGM				70	30	0				80	15	5
MM		/		80	15	5		/		80	20	0
ASGM					/					100	0	0
HC	96	0	4				96	0	4	80	15	5
MSWI	13	86	1	13	86	1	96	0	4	20	60	20
BFLP	100	0	0	80	15	5	100	0	0	80	15	5
BIO	76	5	19	76	5	19	74	5	21		/	
PVC	100	0	0	80	15	5		/				
Total	51	47	2	57	37	6	60	38	2	73	21	6



Table 3 Hg speciation profiles used in provincial and national inventories for typical APCDs (%).

Sources	Hg speciation									
	Provincial inventory			NJU			THU			
	Hg ⁰	Hg ²⁺	Hg ^p	Hg ⁰	Hg ²⁺	Hg ^p	Hg ⁰	Hg ²⁺	Hg ^p	
Coal combustion	ESP	57	41	1	65	35	0	58	41	1
	FF	31	61	7	16	73	11	50	49	1
	WET	65	33	2	30	57	13	65	33	2
	CYC	30	57	14	30	57	13	/		
	ESP+FGD	83	16	0	83	16	0	84	16	1
	SCR+ESP+FGD	71	29	0	72	28	0	74	26	0
	FF+FGD	78	21	1		/		78	21	1
	No	48	34	18	24	20	56	56	34	10
CEM	DPT+DR/FF*	24	75	1	16	73	11	24	76	1
	SKT/ESP*	83	16	1	65	35	0	80	15	5
	RKT/WET*	47	51	1	30	57	14	80	15	5

*: DPT+DR, SKT and RKT for provincial and THU inventory (Zhang et al., 2015); FF, ESP and WET for NJU inventory (Zhao et al., 2015).



Table 4. Uncertainties of Hg emissions in Jiangsu in provincial and national (NJU) inventories by source, expressed as the 95% confidence intervals of central estimates.

	Sources	Hg ^T	Hg ⁰	Hg ²⁺	Hg ^P
Provincial	CPP	(-59%, +147%)	(-64%, +131%)	(-56%, +244%)	(-43%, +418%)
	CEM	(-15%, +58%)	(-36%, +87%)	(-18%, +63%)	(-57%, +218%)
	ISP	(-38%, +53%)	(-33%, +156%)	(-62%, +44%)	/
	OIB	(-52%, +138%)	(-55%, +133%)	(-55%, +146%)	(-67%, +329%)
	Rest sources	(-25%, +133%)	(-20%, +151%)	(-67%, +168%)	(-43%, +367%)
	Total	(-26%, +81%)	(-34%, +99%)	(-23%, +68%)	(-34%, +270%)
NJU	CPP	(-80%, +198%)	(-80%, +198%)	(-80%, +201%)	(-75%, +477%)
	CEM	(-62%, +97%)	(-75%, +140%)	(-63%, +82%)	(-73%, +266%)
	ISP	(-81%, +167%)	(-82%, +157%)	(-82%, +170%)	(-81%, +250%)
	OIB	(-83%, +153%)	(-97%, +218%)	(-97%, +228%)	(-87%, +170%)



FIGURES

Fig. 1. The ratios of estimated Hg emissions for Jiangsu 2010 in global/national inventories to that in provincial inventory for selected sources and anthropogenic total.

Fig. 2. Sensitivity analysis of selected parameters in Hg emission estimation for Category 1 sources. (a) Relative changes in parameters, calculated using Eq. (6); (b) Changes in emissions when parameters in the provincial inventory were replaced with those in other inventories, calculated using Eq. (7). HgC_{raw} : Hg content in raw coal; AL: activity levels as raw coal consumption by CPP and OIB, limestone used by CEM, and crude steel produced in ISP; TA: total abatement rate of APCDs; RR: Hg release rate for combustion; IEF: input emission factors (before control of APCDs); UEF: uniform emission factor (without consideration of different APCD types); EF_{iron} and EF_{steel} : emission factors of pig-iron and steel production respectively.

Fig. 3. Spatial distribution of Hg emissions for Jiangsu 2010 at a resolution of $0.05^{\circ} \times 0.05^{\circ}$ for (a) Hg^T , (b) Hg^0 , (c) Hg^{2+} , and (d) Hg^P .

Fig. 4. Differences in gridded Hg^T emissions in Jiangsu 2010 between provincial and other inventories: emissions in provincial inventory minus those in NJU (a), THU (b), AMAP/UNEP (c) and EDGARv4.tox2 (d). The locations of point sources with relatively large Hg emissions estimated in provincial inventory are indicated in the panels as well.



Fig. 1

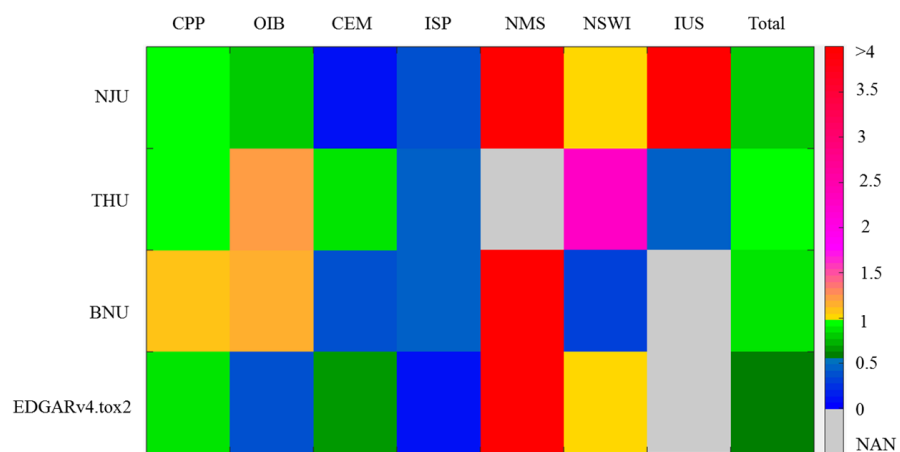




Fig. 2.

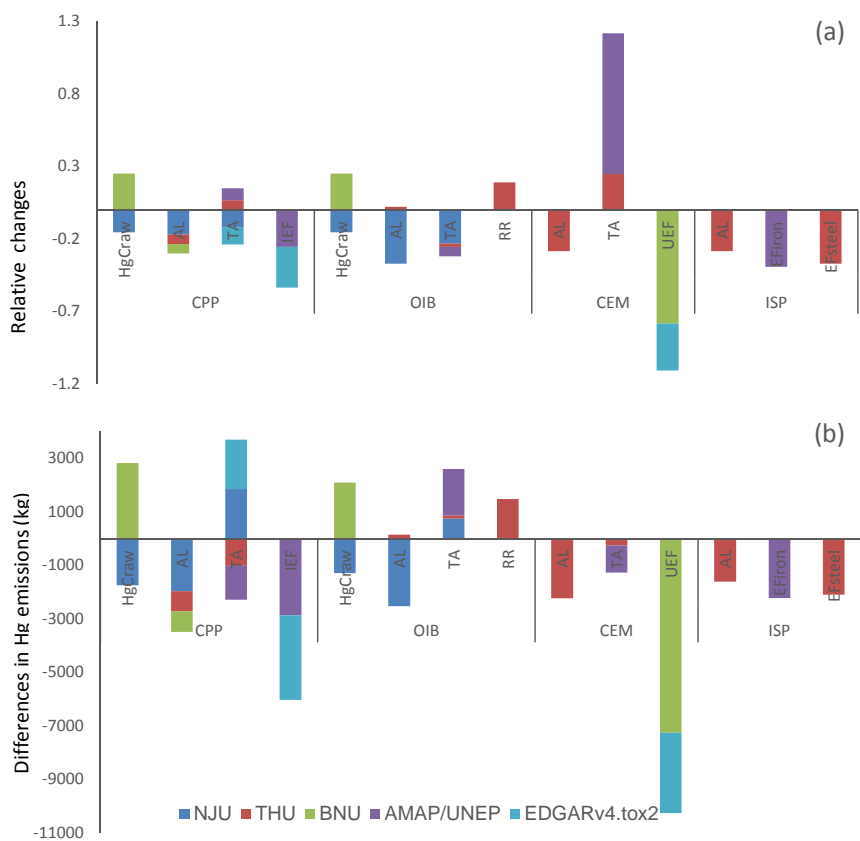




Fig. 3.

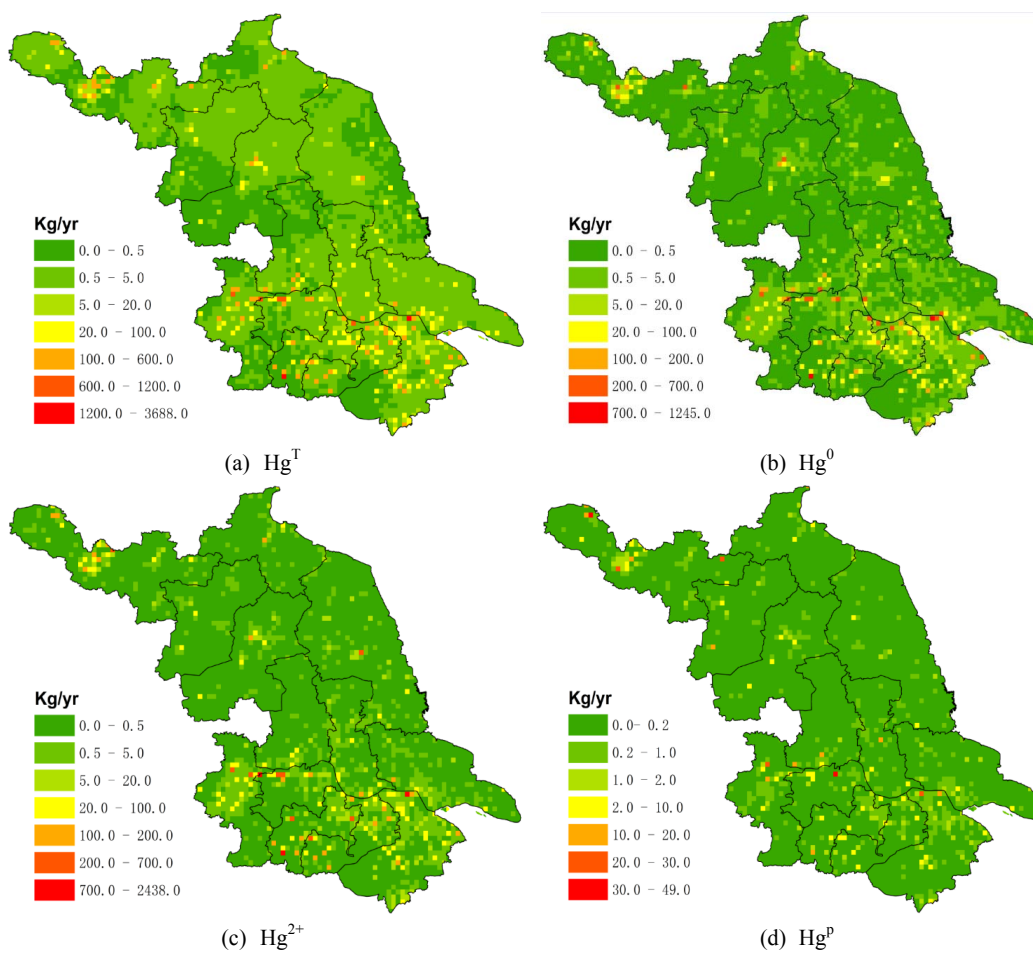




Fig. 4.

